Use of the velocity defect law to assess sand transport rates

Tiago Abreu†, Paulo A. Silva‡, Francisco Sancho∞, Hervé Michallet§

† CESAM & Department of Civil Engineering, Polytechnic Institute of Viseu, ESTV Campus de Repeses, Viseu, 3504-510, Portugal
tabreu@estv.ipv.pt

‡ CESAM & Department of Physics, University of Aveiro, 3810-193 Aveiro, Portugal
psilva@ua.pt

∞ National Civil Engineering Laboratory, Av. do Brasil, 101, Lisboa, 1700-066, Portugal
fsancho@lnec.pt

§ Laboratoire des Ecoulements Géophysiques et Industriels, B.P.53, 38041 Grenoble Cedex 9, France
herve.michallet@legi.grenoble-inp.fr

www.cerf-jcr.org

www.JCRonline.org

ABSTRACT

Abreu, T., Silva, P.A., Sancho, F. and Michallet, H., 2013. Use of the velocity defect law to assess sand transport rates. *In:* Conley, D.C., Masselink, G., Russell, P.E. and O'Hare, T.J. (eds.), *Proceedings 12th International Coastal Symposium* (Plymouth, England), *Journal of Coastal Research*, Special Issue No. 65, pp. 1485-1490, ISSN 0749-0208.

This work uses a simple method based on the defect law that is able to reproduce the horizontal velocities within the wave bottom boundary layer, using a limited number of parameters. The theory is checked against the measured velocity profiles gathered with a high resolution Acoustic Doppler Velocity Profiler. The velocities were collected during an experimental project performed at the Large Oscillating Water Tunnel of Deltares under flat-bed/sheet flow conditions, allowing the analysis of the effects of wave nonlinearities and of a net current on the sediment transport processes. The velocity estimates are used to infer the time-varying bed shear stress, using the momentum-integral method. Secondly, the bed shear stresses are incorporated in a quasi-steady bed load formulation and the transport rate predictions are compared with the net transport rate measurements obtained in the same facility. The results show that the methodology presented in this work provides a suitable estimation of the horizontal near-bed sediment transport rates under non-linear oscillatory flows.

ADDITIONAL INDEX WORDS: *Oscillatory flows, horizontal velocities, defect law, sheet-flow, bed shear stress, sand transport.*

INTRODUCTION

Sediment transport processes are complex since they result from the close interaction between the waves and currents and a mobile bed underneath. A vast amount of work has been done in the past decades to improve our understanding and modeling capabilities concerning sediment transport, but this issue remains a challenge to researchers and much work still needs to be carried out.

In nearshore regions, the wave propagation can induce large horizontal particle displacements near the bottom and, consequently, large horizontal velocities. In order to satisfy the no-slip condition at the seabed, there is a thin region where the wave-induced water motion is strongly influenced by the bed. This layer, called the boundary layer, is characterized by strong velocity gradients, leading to noticeable shear stresses. This region is particularly relevant to sediment transport because it is the place of the mobilization and most of the transport of the sediment particles. It is also within this region of the water column that high levels of turbulence intensities are produced and, consequently, where most of the energy dissipation of the flow occurs. However, accurate measurements of the flow velocity in the bottom boundary layer under oscillatory motions require high-end equipment, sophisticated equipment operation, data protocols and data processing techniques. Therefore, it is desirable to develop theories for estimating the velocity in such flow motions.

The present work uses a simple method based on the defect law (Nielsen, 1992) to reproduce the horizontal velocities within the wave bottom boundary layer, using a limited number of parameters. The theory is checked against the measured velocity profiles gathered with a high resolution Acoustic Doppler Velocity Profiler (Ruessink *et al.*, 2011). The data was collected during an experimental project performed at the Large Oscillating Water Tunnel of Deltares under flat-bed/sheet flow conditions and the experiments highlight the effects of wave nonlinearities and of a net current on the sediment transport processes (Silva *et al.*, 2011). The experimental results are compared with the predictions of a quasi-steady bed load formulation in which the bed shear stress is calculated from the momentum-integral method inferred from the velocity estimates. The results show that the methodology presented in this work provides a suitable estimation of the sediment transport rates.

EXPERIMENTAL SETUP

Facility

Silva *et al.* (2011) performed a set of experiments in the sheet flow regime in the Large Oscillating Water Tunnel (LOWT) of Deltares. The tunnel has the shape of a U-tube with a rectangular horizontal test section and was designed for full-scale simulation of the near-bed horizontal oscillating water motion, which can be combined with a steady current through a recirculation system available in the facility. The desired motion in the test section is created by the vertical movement of a piston in one of the cylinders in the U-tube.

DOI: 10.2112/SI65-251.1 received 07 December 2012; accepted 06 March 2013.

Test Conditions

The experiments considered well-sorted sand with a median diameter d_{50} = 0.2 mm. The test conditions involved different degrees of velocity- and acceleration-skewed flows. The steering signal of the piston followed the general form (Abreu *et al.*, 2010):

$$u_\infty(t) = U_w f \frac{\sin(\omega t) + \frac{r\sin\phi}{1+\sqrt{1-r^2}}}{\left[1 - r\cos(\omega t + \phi)\right]} \quad (1)$$

where $u_\infty(t)$ represents the free-stream velocity, U_w the amplitude of the orbital velocity, ω the angular frequency (= $2\pi/T$), r is a parameter that reflects the index of skewness or nonlinearity ($-1 < r < 1$) and ϕ is a waveform parameter ($-\pi/2 < \phi < \pi/2$). The variable f is a dimensionless factor, function of r ($f = \sqrt{1-r^2}$), allowing the velocity amplitude to be equal to U_w.

The experimental test conditions were divided in three major flow categories: Series A consisted of regular oscillatory flows with different degrees of acceleration skewness; series B considered acceleration-skewed oscillatory flows with a collinear net current, opposing the wave direction; and Series C considered both velocity- and acceleration-skewed oscillatory flows. Table 1 lists the experimental conditions of Series A and C and the corresponding measured time-averaged net transport rates, q_s. Series B will not be considered in this study.

Velocities

In addition to the measurements of sediment transport rates, some of the test conditions considered detailed measurements of time-dependent sand concentrations and flow velocities in the suspension and sheet flow layers, using different kinds of equipment. For the aim of this work, one focuses on the velocity measurements obtained with a high resolution Acoustic Doppler Velocity meter Profiler (ADVP).

The ADVP provided detailed velocity measurements from approximately 150 mm above the bed to within the sheet flow layer, enabling to deduce velocities along the receivers beam axis over a whole profile with a vertical resolution of about 3 mm (Silva et al., 2009). In this work one considers the measured velocity profile time series near the bottom and along the entire boundary layer obtained with the ADVP.

Figure 1 shows the results of the phase-averaged velocities for the oscillatory flow condition A1. At the reference level z = 0 the flow does not present velocities equal to zero. This is due to the development of the sheet flow layer structure that mobilizes fluid and particles at lower levels. In addition, during each experiment, there were some small bed level changes of the order of a few millimeters that were accounted for in the ADVP post processing. The lower plot of Figure 1 also contains the horizontal velocities collected at, approximately, 300 mm above the initial still bed level using an electromagnetic current meter (EMF). This device provides information of the measured free-stream horizontal velocities, $u_\infty(t)$.

The comparison of the velocity time series at the upper level obtained with the ADVP (z = 140 mm) and with the EMF (z = 300 mm) reveals some mismatches around flow reversal. This is probably due to the low seeding at the upper levels (z > 3 cm) during the wave cycle which affects the ADVP measurements (Ruessink *et al.*, 2011). Nevertheless, for lower elevations, one assists to typical features of the wave boundary layer: the velocity magnitude generally increases with distance from the bed with an overshoot velocity within the range z = 10-30 mm and, near the bottom, at different levels, the velocities are not in phase with the free-stream velocity. Additionally, the influence of the acceleration skewness present in test A1 leads to a stronger overshoot velocity and a thinner boundary layer under the positive (onshore) velocities.

Table 1. Experimental conditions and net transport rates (measured values).

Test	U_w (m/s)	T (s)	r (-)	ϕ (rad)	q_s (kg/m/s)
A1	1.32	7	0.28	0.00	0.0539
A2	1.27	10	0.26	0.15	0.0443
A3	1.33	7	0.44	0.00	0.1137
A4	1.29	10	0.45	0.09	0.0847
C1	1.25	7	0.43	-0.93	0.1845
C2	1.35	10	0.42	-0.98	0.2797
C3	1.22	7	0.36	-1.37	0.1244

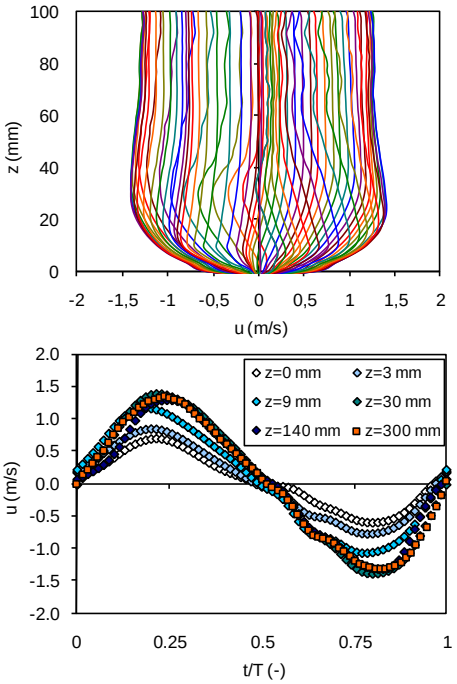

Figure 1. Test A1. a) ADVP phase-averaged velocity profiles; b) Velocity time series at z = 0, 3, 9, 140 mm (ADVP) and at 300 mm (EMF).

METHODS

Velocities and Defect-Law

The velocities $u(z,t)$ inside the wave bottom boundary layer can be written in terms of the free-stream velocity, $u_\infty(t)$, and a velocity defect, $u_d(z,t)$ (Nielsen, 1992):

$$u(z,t) = u_\infty(t) - u_d(z,t). \quad (2)$$

This equation can be written in terms of a dimensionless velocity defect complex function $D_1(z)$:

$$u(z,t) = \left(1 - D_1(z)\right) u_\infty(t) \quad (3)$$

where, for laminar oscillatory flows, $D_1(z)$ follows

$$D_1(z) = \exp\left(-(1+i)\frac{z}{\sqrt{2\nu/\omega}}\right). \quad (4)$$

Here, v is the kinematic viscosity and i is the imaginary unit of complex numbers. It is noted in Eq. (4) that the vertical scale $\sqrt{2\nu/\omega}$ corresponds to the Stokes length. For turbulent flows, Nielsen (1992) suggests a similar expression:

$$D_1(z) = \exp\left(-(1+i)\left(\frac{z}{z_1}\right)^{p_1}\right). \quad (5)$$

where z_1 represents the velocity decay length scale, whereas p_1 is associated to the velocity gradients. As shown by Abreu *et al.* (2012) the parameters z_1 and p_1 are derived from an analysis of the primary harmonic of the velocity records. If z_1 and p_1 adjust well the data, the vertical velocity profile can be estimated with somewhat reduced information. The two parameters allow to obtain $D_1(z)$ through Eq. (5), which combined with $u_\infty(t)$, provide values for $u(z,t)$.

For smooth laminar flows, the real and imaginary parts of the complex logarithm of the defect function are approximately identical along the water column ($\mathrm{Re}\{\ln(D_1(z))\} = \mathrm{Im}\{\ln(D_1(z))\}$, or equivalently, $\ln|D_1(z)| = -\mathrm{Arg}\{D_1(z)\}$). According to Abreu *et al.* (2012), for all the TRANSKEW measurements presented in Table 1, not too close to the bed ($z > 20$ mm), the values of z_1 are within the range 9-10 mm and $p_1 \approx 0.90$. Nevertheless, for lower elevations ($z < 20$ mm), other values can be assumed since the experiments reveal some divergence between $\ln|D_1(z)|$ and $\mathrm{Arg}\{D_1(z)\}$. Following those authors, $D_1(z)$ can be represented by

$$\left|D_1(z)\right| = e^{-(z/0.010)^{0.90}}, \quad (6)$$

$$-\mathrm{Arg}\left\{D_1(z)\right\} = \begin{cases} (z/0.010)^{0.90}, z > 0.021m \\ (z/0.015)^{2.0}, z \le 0.021m \end{cases}. \quad (7)$$

The value of $z = 0.021$ m in Eq. (7) was chosen to guarantee the continuity between the two straight lines with different slopes.

Bed Shear Stress

The velocity profiles within the boundary layer obtained from the defect-law can be used to assess bed shear stresses. Assuming that in the LOWT the free-stream oscillating flow is uniform and parallel to the bed $(\partial u/\partial x \approx 0)$ and that the pressure is constant across the thin bottom boundary layer, it is possible to apply the momentum-integral method to compute the shear stress at a certain elevation z (e.g., Nielsen, 1992; Fredsøe and Deigaard, 1992):

$$\tau(z,t) = \rho\int_z^\infty \frac{\partial}{\partial t}(u_\infty - u)\,dz. \quad (8)$$

where ρ is the fluid density.

The temporal shear stress distributions obtained from Eq. (8) is strongly linked to the free-stream acceleration and the defect function $D_1(z)$. Introducing Eq. (2) into Eq. (8), the shear stress can be rewritten as:

$$\tau(z,t) = \rho\int_z^\infty \frac{\partial}{\partial t}\left(D_1(z)u_\infty(t)\right)dz \quad \Leftrightarrow \tau(z,t) = \rho a_\infty(t)\int_z^\infty D_1(z)\,dz, \quad (9)$$

where $a_\infty(t)$ represents the free-stream flow acceleration.

One notes that Eq. (9) is consonant with Dick and Sleath (1991) observations in the way that the shear stress calculated from this methodology is clearly linked to the pressure gradient, which is proportional to the free-stream acceleration. Nonetheless, Dick and Sleath (1991) noticed in their experiments that there was a phase difference between the shear stress and the acceleration over the sheet flow layer. These results can be justified by Eq. (9) since $D_1(z)$ is a complex function.

Sediment transport

The bed shear stress estimates obtained with Eq. (9) computed at the bottom ($z = 0$) are incorporated into a quasi-steady bedload formula, leading to instantaneous sand transport rates, $q_s(t)$. For that purpose Nielsen's (2006) bedload formulation was adopted, which is a modified version of the Meyer-Peter and Müller (1948) bedload formula:

$$\frac{q_s(t)}{\sqrt{(s-1)g{d_{50}}^3}} = 12\left[\theta(t) - \theta_{cr}\right]\sqrt{\theta(t)}\,\frac{u_*}{|u_*|}, \quad (10)$$

where d_{50} represents the median grain size and the Shields parameter, $\theta(t)=\tau(t)/(\rho(s-1)gd_{50})$, was computed with the shear velocity, u_* $(=\sqrt{\tau/\rho})$. Here, $s = \rho_s/\rho$ is the ratio between sediment and water densities and θ_{cr} is the critical value of θ, at the threshold of motion. A typical value of $\theta_{cr} = 0.05$ was assumed for the present conditions.

It is noticed that the introduction of τ obtained through the momentum-integral for the computation of θ has some shortcomings. This is due to the fact that Eq. (8) does not provide a mean component of τ. Therefore, for combined wave-current motions the proposed methodology is not strictly valid, unless any additional stress is added to Eq. (8), accounting for the current effects.

The analysis of the vertical-cumulative sand transport rate distributions for the experimental conditions in Table 1 lead to the conclusion that most of the sand (60-70%) is transported below $z = 3$ mm (Ruessink *et al.* 2011). Therefore, the majority of the net sand transport rates take place within the sheet flow layer and the use of a bedload formula seems justified.

RESULTS AND DISCUSSION

The combination of the free-stream velocity, $u_\infty(t)$, given by Eq. (1) with $D_1(z)$ enables the reconstruction of $u(z,t)$. Figures 2 and 3 show the results of the predicted velocities according to the defect law for tests A1 and C1, respectively. For comparison, the upper panel also presents the phase-averaged velocities measured with the ADVP. It is noted that the results agree fairly well, showing that the defect law is capable to reproduce the typical features observed in the wave boundary layer: (1) the velocity magnitude generally increases with distance from the bed, (2) at different levels the velocities are not in phase, (3) an overshoot of the velocity occurs at a certain elevation (1-3 cm) above the bed.

Figure 4 and 5 show the time-varying bed shear stresses for tests A1 and C1 computed with the momentum-integral method, using the ADVP velocities, and with the predicted velocities, at the initial bed level ($z = 0$). It can be seen, that the proposed methodology acts as a "low-pass" filter, suppressing the excessive variability resulting from the velocity time derivatives. Though the reconstruction of D1(z) relies only on the 1st harmonic component, the bed shear stress estimates resulting from the defect law closely follow the time-varying trends of the momentum-integral method obtained with the ADVP data, including the positions of the bed shear stress maxima.

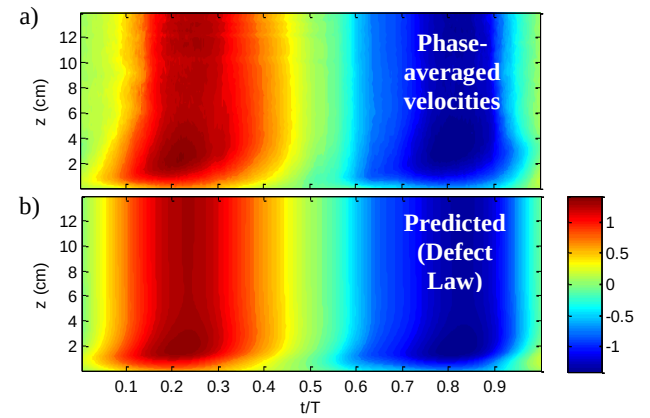

Figure 2. Test A1: a) ADVP phase-averaged velocities (m/s); b) predicted velocities (m/s) according to the defect law.

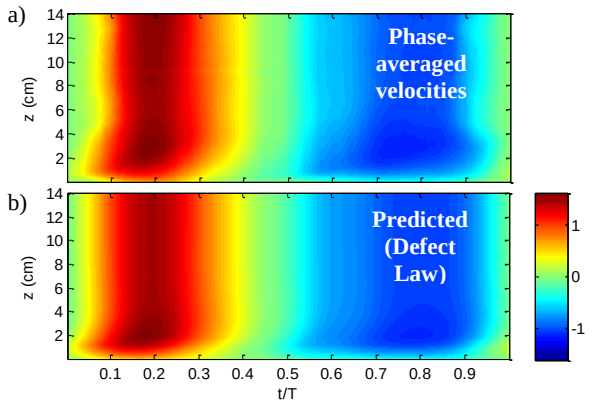

Figure 3. Test C1: a) ADVP phase-averaged velocities (m/s); b) predicted velocities (m/s) according to the defect law.

The lower panels of Figure 4 and 5 shows the instantaneous sand transport rates, $q_s(t)$, in which the bed shear stress has been calculated from the momentum-integral approach, using the predicted velocities for tests A1 and C1. The smooth instantaneous bed shear stresses obtained with the defect law avoid the interference of the fluctuations of τ on $q_s(t)$. It is noted in test A1 that the time-averaged sand transport rate obtained from Figure 4c results in 0.0889 kg/m/s, confirming the magnitude of the value listed in Table 1 for that test condition (q_s= 0.0539 kg/m/s). Such values are, at least, one order of magnitude lower than the instantaneous values in Figure 4c, where the maximum value reaches 1.70 kg/m/s. This result confirms the remarks of Ruessink *et al*. (2011) where the time-averaged sand transport rate, q_s, is a close balance between the net flux during the positive and negative flow phases.

The procedure described above for tests A1 and C1 was adopted for the other test conditions listed in Table 1. Figure 6a shows the comparison between the predicted and measured net transport rates. The oblique non-diagonal lines define a region where the predicted transport is within 50 and 200% of the measured transport. The present methodology can predict almost all the experimental data within a factor of 2. Only test C2 is under predicted by a factor of 3. One points that this particular test presents the highest root-mean-square-value of the oscillatory velocity (=0.94 m/s), whereas the other tests present a practically constant value of 0.88 m/s. Therefore, it is possible that during this test the sand is entrained at higher elevations and the contribution of suspended sand might not be negligible. However, during this test, no detailed measurements of time-dependent sand concentrations and flow velocities were carried out that could support this hypothesis.

Another point that could improve the results concerns the calculation of the mean stress. A stress based on the momentum-integral method does not produce a mean value of τ. However, even for pure skewed and asymmetric flows, i.e., without currents, one expects mean stress values (see for example Fuhrman *et al.*, 2009). Such limitation may be surpassed using simple parameterizations for the computation of the bed shear stress. Recently, Abreu *et al.* (2013) demonstrated how a new formulation to predict the bed shear stress under skewed/asymmetric oscillatory flows (with or without co-linear mean currents) is able to accurately predict sand transport rates when incorporated in the quasi-steady bedload formula used above. Figure 6b shows the results reported in Abreu *et al.* (2013), evidencing the improvement of the results. Nevertheless, the methodology of this study also provides a suitable estimation of the sediment transport rates. In addition, the interesting consistency of z_1 and p_1 for the overall experiments might be very useful. The results obtained from the primary harmonic analysis can be used as input parameters for other bed shear stress parameterizations. For example, Abreu *et al.*'s (2013) formulation requires the knowledge of the bed roughness, k_s, and of a calibrating parameter, φ, that, in the case of a single harmonic, roughly represents the phase lead of the bed shear stress over the free stream velocity. Indeed, the values of z_1 and p_1 are directly linked with k_s and φ. It is noted that, according to Nielsen (1992), the parameters z_1 and p_1 could be prescribed as function of the relative roughness (A/k_s) and the Reynolds number. Therefore, in the future, it would be interesting to investigate such relations in different flow regimes for several experiments.

CONCLUSIONS

In this paper detailed measurements of time-dependent near-bed flow velocities obtained in the Large Oscillating Water Tunnel (LOWT) are analysed. The experiments were performed under sheet flow conditions, contemplating different flow periods and involving different degrees of velocity- and acceleration-skewed flows. The time-dependent flow velocities were obtained with a high resolution Acoustic Doppler Velocity meter Profiler, allowing the application and validation of the velocity defect law. It is seen that the horizontal velocities within the wave bottom boundary layer are accurately reproduced, using a limited number of parameters. The reconstruction of the velocities relies only on the 1st harmonic component and, despite its simplicity, the methodology depicts typical features of the flow within the boundary layer (Figures 2 and 3): (1) the velocity magnitude generally increases with distance from the bed, (2) at different levels the velocities are not in phase, (3) an overshoot of the velocity occurs at a certain elevation (2-4 cm) above the bed.

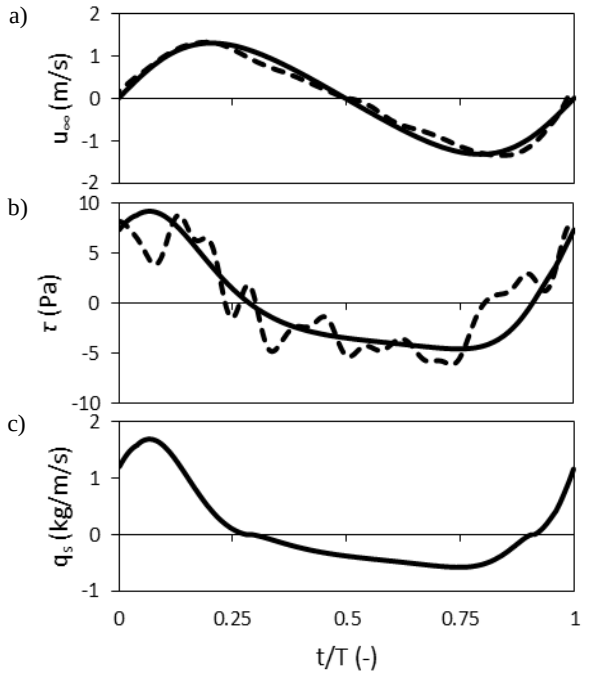

Figure 4. Test A1: a) free-stream velocities following Eq. (1) (solid line) and EMF (dashed line); b) bed shear stresses computed with the momentum-integral method using the ADVP velocities (dashed line) and with the predicted velocities resulting from the defect law (solid line); c) instantaneous sand transport rates.

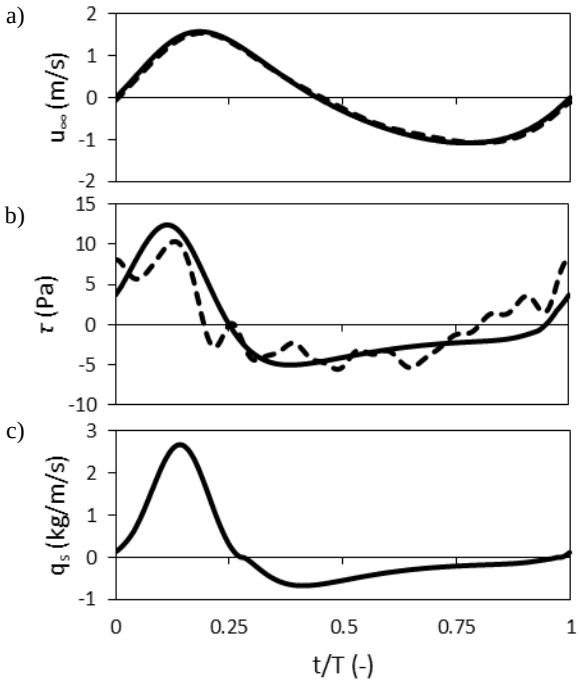

Figure 5. Test C1: a) free-stream velocities following Eq. (1) (solid line) and EMF (dashed line); b) bed shear stresses computed with the momentum-integral method using the ADVP velocities (dashed line) and with the predicted velocities resulting from the defect law (solid line); c) instantaneous sand transport rates.

The velocity estimates are used to infer the time-varying bed shear stress, τ, using the momentum-integral method. Since this methodology does not provide a mean component of τ only tests without superimposed currents were analysed. It is seen that the proposed methodology suppress the undesirable oscillations resulting from the velocity time derivatives and that the bed shear stress estimates, resulting from the defect law, closely follow the time-varying trends of the momentum-integral method obtained with the ADVP data.

The bed shear stresses are incorporated in a quasi-steady bed load formulation and the transport rate predictions are compared with the net transport rate measurements obtained in the same facility. The methodology presented in this work also provides a suitable estimation of the sediment transport rates since practically all data is predicted within a factor of 2. The interesting consistency of the values obtained with the defect law, and particularly, with the analysis of the primary harmonic might be useful in other engineering tools. For example, the values of z_1 and p_1, representative of the velocity decay length scale and with the velocity gradients, respectively, are directly linked with the bed roughness and with the phase lead of the bed shear stress over the free stream velocity. Such parameters are required as input in other practical parameterizations (e.g., Abreu *et al.*, 2013) and, therefore, it justifies a forward-looking analysis on the values of z_1 and p_1.

In the future, a complete validation of the methodology presented earlier would require further measurements of different flow characteristics and other experiments. This simple methodology appears promising in many engineering applications that require the knowledge of the wave boundary layer flow.

ACKNOWLEDGEMENT

The experimental work was supported by the European Community's Sixth Framework Programme through the Integrated Infrastructure Initiative HYDRALAB III, Contract no. 022441(RII3). This work has also been done within the framework of the research projects PTDC/CTE-GIX/111230/2009 (EROS) and PTDC/ECM/103801/ 2008 (3D-MOWADI), supported by the Portuguese Foundation for Science and Technology (FCT).

LITERATURE CITED

Abreu, T., Silva, P.A., Sancho, F. and Temperville, A., 2010. Analytical approximate wave form for asymmetric waves, *Coastal Engineering*, 57, 656-667.

Abreu, T., Silva, P.A., Sancho, F., Michallet, H. and Vasconcelos, L., 2012. Modelling horizontal velocities within the wave bottom boundary layer. *Proceedings of the 23rd IASTED International Conference on Modelling and Simulation* (Banff, Canada), ACTA Press.

Abreu, T., Michallet, H., Silva, P.A., Sancho, F., van der A, D.A. and Ruessink, B.G., 2013. Bed shear stress under skewed and asymmetric oscillatory flows. *Coastal Engineering*, 73, 1-10.

Dick, J.E. and Sleath, J.F.A., 1991. Velocities and concentrations in oscillatory flow over beds of sediment, *Journal of Fluid Mechanics*, 233, 165-196.

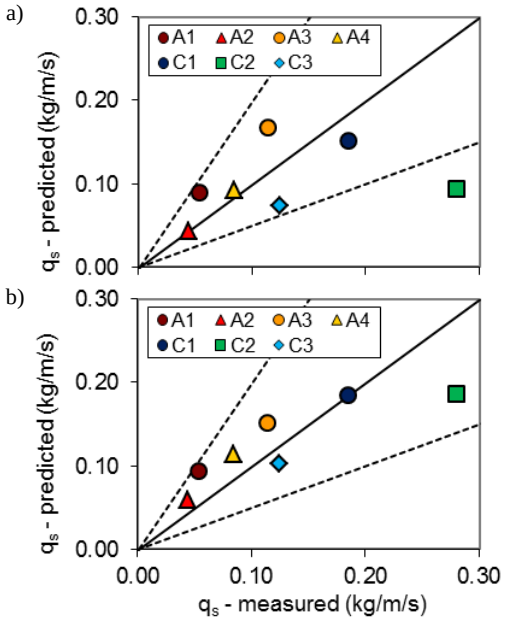

Figure 6. Comparison between predicted and measured net transport rates: a) using the velocities obtained with defect law; b) according to Abreu *et al.* (2013). The solid line corresponds to the perfect agreement between measurements and computations, whereas the dotted lines represent a factor of 2 (and ½) greater (smaller) than the measurements.

Fuhrman, D.R., J. Fredsøe, and Sumer, B.M., 2009. Bed slope effects on turbulent wave boundary layers: 2. Comparison with skewness, asymmetry, and other effects. *Journal Geophysical Research*,114, C03025.

Fredsøe, J. and Deigaard, R., 1992. *Mechanics of coastal sediment transport*. Advanced Series on Ocean Engineering, Volume 3. World Scientific Publication, 369 p.

Meyer-Peter, E. and R. Müller, 1948. Formulas for bed-load transport. *In: Report from the 2nd Meeting of the International Association for Hydraulic Structures Research* (Stockholm, Sweden, IAHR), 39-64.

Nielsen, P. 1992. *Coastal bottom boundary layers and sediment transport*. World Scientific, 324p.

Nielsen, P. 2006. Sheet flow sediment transport under waves with acceleration skewness and boundary layer streaming, *Coastal Engineering*, 53(9), 749-758.

Silva, P.A., Abreu, T., Michallet, H., Hurther, D. and Sancho, F., 2009. Sheet flow layer structure under oscillatory flows. *Proceedings of the 6 IAHR River, Coastal and Estuarine Morphodynamics* (Santa Fe, Argentina), Taylor & Francis, pp. 1057-1062.

Silva, P.A., Abreu, T., van der A, D.A., Sancho, F., Ruessink, B.G., van der Werf, J.J. and Ribberink, J.S., 2011. Sediment transport in non-linear skewed oscillatory flows: Transkew experiments, *Journal of Hydraulic Research*, 49, sup1: 72-80.

Ruessink, B.G., Michallet, H., Abreu, T., Sancho, F., van der A, D.A., van der Werf, J.J. and Silva, P.A., 2011. Observations of velocities, sand concentrations, and fluxes under monochromatic velocity-asymmetric oscillatory flows, *Journal of Geophysical Research*, 116, C03004.